Mechanistic Insights into Human Antimicrobial Peptide-Induced Activation of a Broadly Conserved Bacterial Signaling System

Samuel A. Adeleye[1], Abraham F. Mechesso[2], Arpita Mukherjee[1], Guangshun Wang*[,2], Srujana S. Yadavalli[1]*

[1]Waksman Institute of Microbiology and Department of Genetics, Rutgers University, Piscataway, New Jersey 08854 USA

[2]Department of Pathology and Microbiology, College of Medicine, University of Nebraska Medical Center, Omaha, Nebraska 68198 USA

*Corresponding authors: sam.yadavalli@rutgers.edu, gwang@unmc.edu

Short title: Peptide-induced activation of a bacterial signaling system

Keywords: Bacteria, antimicrobial peptides, two-component signaling systems, stress response, cell elongation, reporter gene assays

Abstract

Antimicrobial peptides (AMPs) represent a promising class of therapeutics against bacterial pathogens. While their direct bactericidal mechanisms are well-characterized, how bacteria sense and respond to these peptides at sublethal concentrations remains poorly understood. Here, we investigate the activation of the *Escherichia coli* PhoQ-PhoP signaling system by the human cathelicidin LL-37 and its derivatives (KR-12 and RI-10). We demonstrate that these peptides exhibit variable antimicrobial potency but surprisingly similar abilities to activate the PhoQ-PhoP pathway, indicating that signaling function is separable from bactericidal activity. Notably, sublethal concentrations of these peptides induce significant cell elongation, a phenotype dependent on PhoQ and mediated by the upregulation of QueE, which interferes with bacterial cell division. Contrary to the previous model suggesting peptides activate PhoQ passively by displacing its inhibitor MgrB, we observed enhanced cell elongation in *ΔmgrB* strains across all tested peptides, including RI-10, lacking antibacterial activity. Our findings suggest peptides actively stimulate PhoQ through a mechanism independent of MgrB dissociation, providing a more refined understanding of the peptide signaling through the PhoQ-PhoP system. These insights into bacterial adaptation mechanisms against host-derived peptides may guide the development of peptide therapeutics with enhanced efficacy against drug-resistant pathogens.

48 ## Introduction

49 When exposed to specific cationic antimicrobial peptides (AMPs) at sublethal concentrations,
50 *Escherichia coli* activates the PhoQ/PhoP signal transduction pathway—a conserved two-
51 component system crucial for stress adaptation in Gram-negative bacteria (1, 2). The
52 PhoQ/PhoP signaling system is also an important pathway for adaptation and survival in
53 conditions such as low Mg^{2+}, mildly acidic pH, and hyperosmolarity in *E. coli* and closely related
54 enterobacteria (3, 4). Activated PhoQ-PhoP regulate numerous genes, including those
55 responsible for remodeling the outer membrane, activation of efflux pumps, and proteolytic
56 degradation of the peptides that help bacteria resist cationic AMPs (5–8). Strong activation of
57 the PhoQ-PhoP system is observed when cells are treated with a human platelet-derived AMP
58 (C18G), causing the upregulation of QueE, an enzyme primarily known for its role in the
59 queuosine biosynthetic pathway that modifies specific tRNAs (2). Remarkably, elevated QueE
60 levels lead to the accumulation of this protein at the bacterial division septum, where it interacts
61 with the cell division machinery. This interaction disrupts normal septation processes
62 downstream of Z-ring formation, resulting in inhibited cell division and the development of
63 filamentous bacterial morphology. This mechanism represents a sophisticated bacterial stress
64 response that temporarily halts proliferation when facing host antimicrobial challenges.
65
66 Human cathelicidin, LL-37, is one of the best-studied AMPs (9–11) with a broad spectrum of
67 activity against bacteria, fungi, parasites, viruses, and cancer cells (11–15). LL-37 is known to
68 activate the PhoQ-PhoP system and exert its antimicrobial action primarily by interacting with
69 bacterial membranes, inserting itself into the lipid bilayer, and leading to membrane
70 destabilization and the formation of pores (1, 16–18). This disruption results in the loss of
71 membrane integrity, causing leakage of cellular contents and ultimately leading to bacterial cell
72 death. LL-37's efficacy against pathogens is influenced by the composition of the growth

73 medium, particularly the presence of high salt concentrations and divalent cations (19). In our
74 current understanding, cationic antimicrobial peptides interact with the acidic patch in the
75 periplasmic sensing domain of PhoQ, displacing divalent cations (particularly Mg^{2+}) that
76 normally repress PhoQ activity, leading to PhoQ autophosphorylation and subsequent
77 phosphorylation of PhoP (1). Besides peptides and other signals, a 47 amino acid long small
78 membrane protein called MgrB interacts with and inhibits PhoQ by affecting its kinase activity
79 (20, 21). Specific residues in the transmembrane and periplasmic regions of MgrB are important
80 for the interaction with PhoQ (22). It is proposed that the sensing of AMPs by PhoQ at
81 physiological concentrations of magnesium is dependent on MgrB (23). A conformational
82 change in PhoQ upon AMP binding is thought to disrupt the PhoQ-MgrB complex, resulting in
83 PhoQ activation via derepression. This model suggests that AMPs play an inert role in
84 stimulating PhoQ.
85
86 Human cathelicidin LL-37 contains 37 amino acids and is costly to make. Structural studies
87 established that the C-terminal tail of LL-37 (residues 33-37) is disordered and not required for
88 membrane-targeting mediated antimicrobial activity (24). This led to the use of several
89 derivatives of the LL-37 peptide from the central region for therapeutic development (11, 24, 25).
90 KR-12, the smallest antibacterial peptide of human LL-37 (24), has been widely utilized in
91 peptide engineering (26). To effectively develop AMPs as novel peptide therapeutics, it is
92 imperative to study the bacterial response to these peptides, including the biochemical and
93 regulatory pathways that underlie this process. While there has been tremendous progress in
94 establishing the direct antimicrobial action of AMPs (27), much less is known about the
95 phenotypic responses elicited by AMPs at sub-lethal doses and whether the peptides have a
96 direct and active effect on stimulating PhoQ.
97

98 In this study, we first examined the antibacterial activity of LL-37 and its smaller fragments, KR-
99 12 and RI-10, to establish their minimum inhibitory concentration (MIC) and minimum
100 bactericidal concentration (MBC) against *E. coli* under physiologically relevant growth
101 conditions. We then determined the killing kinetics and characterized the peptides using
102 membrane permeabilization and depolarization assays. Next, we investigated whether LL-37
103 and its derived peptides, at concentrations below MIC, are effective in activating the PhoQ/PhoP
104 signaling system by analyzing both the changes in cell morphology and PhoP-dependent
105 transcriptional reporter activity as readouts. Finally, using cells lacking the PhoQ inhibitor, MgrB,
106 we provide key insights into how LL-37 and its derivatives may interact with their target histidine
107 kinase and affect bacterial physiology. Our study sheds light on the mechanism of molecular
108 regulation of bacterial physiology by biologically relevant host defense peptide LL-37, which is
109 known to play a key role in human health via both antimicrobial and immune regulatory roles (9-
110 12,27).
111

112 ## Results

113 **Analysis of LL-37 and its derivatives for antibacterial activity against *E. coli*.**
114 To assess the antibacterial activity of AMP LL-37 derivatives KR-12 and RI-10 against *E. coli*,
115 we compared the minimum inhibitory concentration (MIC) or minimum bactericidal concentration
116 (MBC) to establish the lowest concentration of LL-37 or its derivatives that either inhibit growth
117 or kill the cells, respectively. Thus, lower MIC and MBC values indicate higher potency of the LL-
118 37 or its derivatives. To better delineate antimicrobial capability, we evaluated the activity of LL-
119 37 and its derivatives in three different media conditions, Mueller Hinton Broth (MHB), tryptic
120 soy broth (TSB), or supplemented minimal A medium (MinA) against four *E. coli* strains
121 (MG1655, E423-17, E416-17, and 25922, Tables 1, S1, S2). Gentamicin was included as a non-
122 peptide antibiotic control. LL-37 exhibited the highest potency with MIC values around 2-8 μM,

123 depending on the media used (Table 1). Interestingly, the KR-12 peptide, which is shorter than
124 LL-37 by 25 amino acids, is also active against the *E. coli* isolates tested. The MIC and MBC
125 values for KR-12 are similar or 2-4 fold higher than those obtained for LL-37. The values
126 obtained in minimal medium were in a similar range as those obtained in other media, especially
127 for *E. coli* K-12 MG1655 strain (Tables 1, S1). The shortest LL-37 variant, RI-10, did not show
128 antibacterial activity against any of the isolates tested here across different media conditions, or
129 after dilution of MHB to 10%. From here on, for characterization of the antibacterial and
130 physiological effects of these peptides, we used the *E. coli* MG1655 strain grown in
131 supplemented minimal medium. Next, we investigated the time-dependent killing kinetics of LL-
132 37, KR-12, and RI-10 to further substantiate their bactericidal properties using a concentration
133 corresponding to 2x MIC values (Figure S1). LL-37 (2× MIC) completely eradicated the
134 exponential phase of *E. coli* K-12 MG1655 in 1 hour, while KR-12 caused about a 4-log fold
135 reduction in 2 hours. As expected, RI-10 displayed no activity at the concentration tested.
136 Together, these results show that full-length LL-37 and KR-12 exhibit antibacterial properties
137 against *E. coli* but not RI-10.
138
139 **LL-37 and KR-12, but not RI-10, disrupt bacterial membranes.**
140 Given that LL-37 and its derivative SK-24 both target bacterial membranes, we wondered if the
141 shorter peptide variants, KR-12 and RI-10, may retain and exhibit activity against *E. coli*
142 membranes. To assess membrane disruption, we conducted membrane permeabilization and
143 depolarization experiments. We analyzed membrane permeability by the uptake of a
144 membrane-impermeable red dye, propidium iodide (PI), either in the presence of a peptide,
145 0.1% Triton-X (positive control) or PBS (untreated). Treatment with either LL-37 or KR-12 led to
146 an increase in membrane permeability in a dose-dependent manner, although LL-37 was more
147 effective (Figure 1A-C). To assay membrane depolarization, we used $DiBAC_4(3)$, a probe for
148 membrane potential, whose fluorescence increases upon entering depolarized cells. As

149 expected, LL-37 depolarized membranes well with increasing concentration of the peptide
150 (Figure 1D-F). Similarly, KR-12 also caused membrane depolarization but to a lower extent
151 relative to LL-37. Consistent with the data from MIC assay and killing kinetics, RI-10 did not
152 have a discernible effect on membrane permeability and depolarization. Together, the data
153 suggest that KR-12, like LL-37, targets the bacterial membrane as its mode of action.
154
155 **Sub-MIC levels of LL-37 and KR-12 activate the PhoQ/PhoP signaling system and cause**
156 **cell elongation.**
157 Cationic antimicrobial peptides, LL-37 and C18G activate the PhoQP pathway in *E. coli* and
158 related bacteria (1, 2). In addition, *E. coli* cells elongate upon exposure to a sub-lethal dose of
159 C18G, leading to filamentous growth (2). This filamentation is associated with conditions that
160 strongly activate PhoQ/PhoP. We asked if the truncated LL-37 derivatives retain the ability to
161 activate the PhoQP system. We used a promoter-reporter strain containing P_{mgrB}-*yfp* to measure
162 the transcriptional activity of the *mgrB* gene, whose expression is PhoQP-dependent. In parallel,
163 we observed the cells by phase contrast microscopy to test if the peptides induce any changes
164 in *E. coli* cell morphology. Our analysis revealed that there is a 3 to 3.5-fold increase in PhoQP-
165 regulated transcriptional activity when cells are treated with a sub-MIC dose of LL-37 at 1.25 μM
166 and KR-12 at 5 μM (Figure 2A). RI-10 showed weak activation of ~1.7-fold higher than the
167 untreated control. As the amino acid sequence of RI-10 is included in both KR-12 and LL-37, we
168 also asked how a different LL-37 segment, KE-10, with a minimal sequence overlap with KR-12
169 and RI-10 (Table S2), behaves. Like RI-10, KE-10 showed no antibacterial activity against *E.*
170 *coli* (MIC > 64 μM in Table 1). In contrast to RI-10, the KE-10 peptide showed negligible
171 activation of the PhoQP system based on the transcription activity measurement of the *mgrB*
172 gene, implying that there is a requirement for a particular peptide sequence for this activation.
173 Although LL-37 was long known to activate the PhoQP system, its impact on *E. coli* cell
174 morphology, especially at concentrations below the MIC, has not been studied previously. Upon

175 observation by phase contrast microscopy, both LL-37 and KR-12 treated cells displayed
176 elongation with heterogeneous cell lengths (Figure 2B). The average cell lengths increased by
177 ~1.5-fold for cells exposed to LL-37 and KR-12 when compared to the control cells (Figure 2C).
178 However, both RI-10 and KE-10 treated cells did not show a significant change in cell length
179 (Figure 2B-C). Together, these data elucidate that the truncated LL-37 derivative KR-12, but not
180 RI-10, is functional in stimulating the PhoQP pathway and eliciting a physiological response.
181 Additionally, our findings indicate that this stimulation by full-length LL-37 and its minimal
182 antibacterial peptide KR-12 is strong enough to cause morphological changes similar to what
183 was observed for the C18G peptide previously (2) , whereas two shorter LL-37 segments, which
184 lost antibacterial activity, were unable to.
185
186 **Cell elongation caused by sub-MIC levels of peptides is dependent on PhoQ and QueE.**
187 Given that sub-lethal concentrations of AMPs LL-37 and KR-12 stimulate the PhoQP signaling
188 pathway, we examined the morphology of the cells upon deletion of *phoQ*. As expected, Δ*phoQ*
189 cells did not elongate when treated with LL-37 and KR-12 (Figure 3A). There was no increase in
190 PhoQP-dependent transcriptional activity of P_{mgrB}, even in the presence of LL-37 and KR-12 in
191 Δ*phoQ* cells (Figure 3B), and the average cell lengths were similar relative to the no-peptide
192 control (Figure 3C), confirming that the cell elongation phenotype associated with these AMPs is
193 dependent on PhoQ activation. In previous work, sub-MIC levels of C18G are shown to cause
194 filamentation in wild-type *E. coli* cells, which is mediated by increased expression of a PhoP-
195 dependent gene called *queE*, encoding a protein with dual activities in the inhibition of cell
196 division and the synthesis of queuosine tRNA modification (2, 28). We asked if the
197 morphological phenotype observed here for cells exposed to LL-37 and KR-12 is also mediated
198 by QueE or through an independent mechanism. Using a *queE* deletion strain, we carried out
199 microscopy and measured cell lengths and transcriptional reporter activity. Δ*queE* suppressed
200 the elongation phenotype observed when cells were treated with either LL-37 or KR-12 (Figures

201 3A, 2B). It is worth noting that Δ*queE* cells grown in the presence of these peptides still display
202 an increase in PhoQP-regulated transcriptional reporter activity similar to the wild-type cells
203 (Figures 3D, 2A). Consistently, Δ*queE* cells exposed to peptides did not show a difference in the
204 average cell length relative to the controls (no peptide, RE-10, Figure 3E). Overall, filamentation
205 and heterogeneity in cell size observed upon treatment with LL-37 and KR-12 peptides are both
206 PhoQ- and QueE-dependent.
207
208 **Deletion of PhoQ inhibitor, MgrB, increases cell responsiveness to LL-37 and its**
209 **derivatives.**
210 Cells deleted for MgrB show an overall, robust increase in PhoQP-controlled gene expression
211 (20). These cells experience higher stimulation of PhoQ under magnesium-limiting conditions,
212 similar to the strong activation of this system observed in wild-type cells grown in the presence
213 of C18G at intermediate magnesium concentrations (2). Consequently, Δ*mgrB* cells grow as
214 long filaments, and this phenotype is dependent on upregulation of QueE expression by
215 PhoQ/PhoP (2). It is proposed that MgrB mediates the sensing of specific AMPs by PhoQ at
216 intermediate concentrations of magnesium, therefore, LL-37, KR-12, and RI-10 may activate
217 PhoQ only when MgrB is present. In this case, we expect Δ*mgrB* cells to show no significant
218 change in either the PhoP-dependent transcriptional reporter activity or cell morphology when
219 treated with peptides vs. no treatment. We examined how LL-37 and its derivatives influence the
220 activity of the PhoQP system and cell lengths in a Δ*mgrB* strain. As expected, in the absence of
221 peptides, Δ*mgrB* cells showed an increase in P_{mgrB} transcription relative to the wild-type cells
222 under the same growth conditions (Figures 4A, 2A). When the AMPs were added to Δ*mgrB*
223 cells, there was a modest increase of ~1.4-fold in the PhoQP-regulated transcriptional reporter
224 activity for LL-37, as observed previously using the same media conditions carrying 0.1 mM
225 Mg^{2+} (Figure 4A) (20). The addition of peptides KR-12, RI-10, and KE-10 did not lead to a
226 substantial increase in reporter activity, suggesting that PhoP-mediated transcription is not

227 sensitive in response to the two peptides in cells lacking MgrB. This result is consistent with a
228 recent study where Δ*mgrB* cells did not show an increase in PhoP-regulated transcription in the
229 presence of another AMP, C18G (23).
230 To investigate this further, we analyzed the morphology of Δ*mgrB* cells in the presence of
231 peptides, wherein cell elongation is PhoQ-dependent and a direct function of strong PhoQP
232 activation. As expected, we noticed filamentation in Δ*mgrB* cells treated with LL-37 and KR-12,
233 but only short, typical cells in the KE-10-treated or no-peptide control cells, under this growth
234 condition with 0.1 mM Mg^{2+} (Figure 4C). It was intriguing, however, to see that RI-10-treated
235 Δ*mgrB* cells also displayed elongation, suggesting that RI-10 may interact more effectively with
236 PhoQ to activate it, in the absence of MgrB. In other words, loss of the inhibitor MgrB appears to
237 unmask the effect of RI-10 peptide on PhoQ stimulation, resulting in an evident cell elongation
238 phenotype. Interestingly, cell size quantification revealed greater heterogeneity and higher
239 average cell lengths across all three peptides for Δ*mgrB* of 6-8 μm (Figure 4D). The mean cell
240 lengths for LL-37, KR-12, and RI-10-treated Δ*mgrB* cells were higher than the corresponding
241 values obtained for the wild type by 2.5-, 2.3-, and 1.9-fold, respectively; however, there is no
242 difference in cell length in the KE-10-treated cells (Figures 4D, 2C), indicating a central role of
243 the RI-10 containing LL-37 segments in activation in the absence of *mgrB*.
244 It is known that high stimulation of PhoQ from exposure to LL-37 results in differential regulation
245 of specific PhoP-regulated promoters, including that of *mgrB* (29). Also, upon activation by LL-
246 37, a mutated *mgrB-t7a* promoter (with a T7A substitution in the PhoP-binding site) shows a
247 higher fold change in transcriptional activity relative to the wild-type *mgrB* promoter. To
248 substantiate whether there may be an increased transcriptional response to peptide treatment
249 via this promoter, we analyzed wild-type and Δ*mgrB* strains carrying the *mgrB-t7a* promoter
250 (Figure S2). We observed a significant increase in cell size heterogeneity in wild-type cells
251 treated with LL-37 and KR-12, and Δ*mgrB* cells treated with LL-37, KR-12, and RI-10. The cells
252 did not display an increase in cell lengths when treated with control peptide KE-10 or in the

253 absence of a peptide. Together, these data support the idea that LL-37 and its derivatives
254 potentially compete with MgrB to bind and activate PhoQ, and when MgrB is absent, the AMPs
255 and other peptides can further activate PhoQ. If the exacerbated cell elongation observed in
256 peptide-treated Δ*mgrB* cells is indeed due to a PhoQP-dependent mechanism that is mediated
257 by QueE, we should see this phenotype suppressed upon deletion of *queE*. Consistent with our
258 hypothesis, Δ*mgrB* Δ*queE* cells treated with LL-37, KR-12, and RI-10 displayed a loss of
259 filamentation and a decrease in cell size heterogeneity (Figure 4D).
260

261 ## Discussion

262 Despite extensive investigation, fundamental questions remain about the molecular
263 mechanisms of peptide-mediated signal transduction by the PhoQ-PhoP system. Moreover, the
264 effects of PhoPQ activation by these AMPs in cells and the physiological importance of these
265 interactions have not been elucidated. We address two critical questions in this work: (i) Can
266 peptides lacking potent antimicrobial activity still interact with PhoQ and act as a signal for this
267 pathway? Using LL-37 and derivatives with variable MICs and antibacterial activities against *E.*
268 *coli* cells, we show that the signaling function of peptides through the PhoQ-PhoP system is
269 separable from their antimicrobial activity (Figure 5A), suggesting that bacteria may use this
270 pathway primarily as a detection mechanism for host environments rather than simply as a
271 response to membrane damage. (ii) Do the peptides actively stimulate PhoQ, or do they exert
272 their effect on PhoQ passively by displacing the inhibitor protein, MgrB? Many studies on
273 peptide-induced signaling of PhoQ measure the activity of peptides using PhoP-dependent
274 transcriptional reporters as a proxy. In agreement with the previous studies, upon exposure to
275 peptides, we do not observe a significant increase in PhoQP-driven transcriptional reporter
276 activity in *ΔmgrB* cells relative to the wild type. It is possible that the derepression of PhoP-
277 regulated gene expression in the absence of MgrB could lead to lower sensitivity of the reporter

278 signal, masking small increments in the amplitude. While such reporters are incredibly useful in
279 determining the activation status of this pathway and measuring the transcription levels, we
280 have a second, sensitive readout – a cell elongation or filamentation phenotype in response to
281 peptide stress in *E. coli*. Based on our microscopy and cell length measurements, we find that
282 cells elongate significantly upon exposure to sublethal concentrations of peptides, LL-37 and
283 KR-12, even though the promoter reporters do not show a significant change in their activities.
284 The extent of cell elongation may differ in response to specific peptides, as we note that
285 filamentation induced by an AMP, C18G, in wild-type *E. coli* cells is quite robust, with an
286 average cell length of > 20 μm (2). Upon deletion of MgrB, the average cell lengths increased
287 further, and even RI-10-treated cells displayed cell elongation; this observation is in stark
288 contrast to a previous model suggesting that AMPs activate PhoQ by driving the dissociation of
289 MgrB (23). Our findings elucidate phenotypic effects on cell size caused by the peptides in a
290 PhoQ-dependent manner and implicate an active and more direct role for peptides in PhoQ
291 activation (Figure 5B).
292
293 Our understanding of what characteristics of AMPs are required to activate the PhoP-PhoQ
294 system is still evolving. A previous report found a correlation between the extent of positive
295 charge, hydrophobicity, and amphipathicity of an AMP and its ability to activate PhoQ-PhoP (8).
296 Intriguingly, the authors discovered that even a peptide with minimal positive charge (+1) but
297 containing histidines was highly potent at activating the system, suggesting the existence of an
298 activation mechanism independent of peptide charge. A later study with 117 AMPs from the
299 Antimicrobial Peptide Database (30) showed that PhoQ is activated by a diverse set of AMPs,
300 including the human cathelicin LL-37 and non-cathelicidin peptides that carry either an α-helical
301 or a combination of α-helical/β-sheet structural regions (31). In our work, we see that LL-37
302 derivatives induce PhoQ-dependent morphological changes, and KR-12, the smallest
303 antibacterial peptide, is also the smallest peptide sequence for the PhoPQ induction. Further,

304 RI-10, but not KE-10, became responsive upon the deletion of mgrB. Interestingly, LL-25, the
305 N-terminal segment of LL-37 which does not kill bacteria under normal conditions (31), does not
306 activate PhoPQ based on the recent human AMPs screen study although it contains partial
307 sequence of KR-12 (30). LL-25 can be obtained by extending the sequence of KE-10 from both
308 ends (Tables S2, S3). Thus, our study implies that the bacterial molecular detection machinery
309 is elegantly tuned to specifically target the minimal antimicrobial region of human antimicrobial
310 peptide LL-37 but not fragments outside the region. Biologically, bacterial targeting of the key
311 antimicrobial region of human LL-37 (24) is rather effective since this region is commonly
312 shared by all the active fragments of LL-37 naturally produced in human skin (Table S3),
313 including KS-27, KR-20, KS-30, RK-31, and LL-29 (32). Indeed, all these human fragments
314 responded to the PhoPQ system based on a recent screening of human AMPs registered in the
315 APD (30). Collectively, these findings indicate that the PhoQ-PhoP system likely responds to
316 peptides based on specific structural and chemical properties rather than simply their
317 antimicrobial activity, allowing bacteria to sense and respond to host environments in a more
318 nuanced way than just reacting to membrane damage.
319
320 Finally, the dramatic rise of antimicrobial resistance is a major public health concern. AMPs and
321 other peptide derivatives are relatively small, typically comprised of around 10 to 50 amino acids
322 (30), and constitute a key component of host innate immunity for defense against microbial
323 pathogens (32, 33). These peptides are relatively cheap to produce, have good thermal stability
324 and water solubility, and exhibit a broad spectrum of activity against bacteria and fungi, making
325 them promising candidates for drug development (34–38). Studying the cellular responses to
326 AMPs and peptides in general provides us with a deeper understanding of how cells can sense,
327 adapt, and develop tolerance to these molecules and guide the strategic design of therapeutics
328 with enhanced efficacy.
329

330 # Materials and Methods

331 **Strains**

332 Details of the strains used in this study are provided in Table S4. AML20, JNC21, NRS5, NRS6,
333 SAM31, TIM92, TIM100, and TIM166 are *E. coli* K-12 MG1655 derivatives. Additionally, clinical
334 strains of *E. coli*, E423-17, E416-17, and ATCC strain 25922 were used for specific assays as
335 indicated. NRS6 was made by transducing the KEIO strain JW1815 into the TIM148 and
336 TIM166 strains, respectively, using $P1_{vir}$.

337

338 **Media, reagents, and growth conditions**

339 Routine bacterial growth on solid agar was performed using LB Miller medium (IBI scientific)
340 containing 1.5% bacteriological grade agar (VWR Lifesciences) at 37°C. Liquid cultures were
341 grown at 37°C with aeration in either LB miller medium or minimal A medium (MinA) (39)
342 (K_2HPO_4 (10.5 g l^{-1}), KH_2PO_4 (4.5 g l^{-1}), $(NH_4)_2SO_4$ (1.0 g l^{-1}), Na_3 citrate.$2H_2O$ (0.5 g l^{-1}),
343 supplemented with 0.1% casamino acids, 0.2% glucose and 1 mM $MgSO_4$ unless otherwise
344 indicated. Throughout this study, supplemented MinA, as indicated above, will be referred to as
345 a minimal medium. In addition, Mueller-Hinton broth (MHB, catalog info) and tryptic soy broth
346 (TSB, catalog info) were used for minimum inhibitory/bactericidal concentration (MIC/MBC)
347 assays. Peptides and/or AMPs used in the study are indicated in Table S2.

348

349 For the measurement of cell length and transcriptional reporter activity, overnight cultures of
350 SAM31, TIM92, TIM100, AML20, SAA58, and JNC21 were grown in supplemented MinA
351 containing 1 mM $MgSO_4$. Saturated cultures were back diluted 1:500 into 5 ml supplemented
352 MinA with 0.1 mM Mg^{2+} and grown for 2 hours in a shaker at 300 rpm. Each culture was split
353 into two tubes, with one tube designated as a no-peptide control and the second tube where a
354 test peptide was added. LL-37, KR-12, RI-10, and KE-10 were added to a final concentration of

355 1.25 μM, 5 μM, 5 μM, and 5 μM, respectively. These cultures were further grown for 4 hours at
356 37°C in a roller drum at 60 rpm.
357
358 **Microscopy and image analysis**
359 Cell morphology was observed and single-cell fluorescence to measure transcriptional reporter
360 activity was performed using phase contrast and fluorescence microscopy as previously
361 described (2). 3 μl of the cells were immobilized on a 1% agarose pad and observed using a
362 Nikon TiE fluorescent microscope with a TI2-S-HU attachable mechanical stage and a perfect
363 focus system (PFS). The images were captured using a Teledyne Photometrics Prime 95B
364 sCMOS camera with 1x1 binning. YFP and CFP fluorescence was imaged using a 100 ms
365 exposure time at 20% intensity. Image acquisition was done using Metamorph software version
366 7.10.3.279 (Molecular Devices, Sunnyvale, CA). The background fluorescence was determined
367 using MG1655 cells grown under the same conditions. The average cell fluorescence was
368 quantified using ImageJ (40) and the MicrobeJ plugin (41). Data from independent replicates
369 was plotted using R.
370
371 **Minimum inhibitory/bactericidal concentration (MIC/MBC) testing**
372 The antibacterial activity of the peptides against *E. coli* MG1655, E423-17, E416-17, and 25922
373 strains was evaluated using a previously established protocol (42). Briefly, a peptide
374 concentration gradient with twofold dilution was prepared in the 96-well polystyrene microplate
375 at 10 μl per well. Bacteria were grown to the exponential phase in MHB, TSB, or supplemented
376 MinA. It was then diluted to ~10^5 CFU/ml in MHB, TSB, or supplemented MinA with 0.1 mM
377 $MgSO_4$, and partitioned into the 96-well microplate at 90 μl per well. After overnight incubation at
378 37°C, readings were taken at 600 nm using a ChroMate 4300 Microplate Reader at (GMI,
379 Ramsey, MN). The minimum inhibitory concentration (MIC), represented as ranges, was
380 determined for wells without bacterial growth. For minimum bactericidal concentration (MBC)

381 determination, aliquots of 30 µl from growth-absent wells were plated on MH agar plates, and
382 the lowest peptide concentration with no isolated colony was considered the MBC. Results were
383 expressed in µM.
384
385 **Membrane permeabilization**
386 The peptide ladder was prepared as described for the antibacterial assay in a black COSTAR
387 96-well plate. Propidium iodide (PI) (MP Biomedicals, Solon, OH) was prepared in the dark and
388 dissolved in DMSO (Thermo Fisher Scientific, NY) to 20 mM. This PI stock solution was further
389 diluted to 1 mM with water and 2 µl of 1 mM PI was added to each well. An overnight culture of
390 *E. coli* K12 MG1655 was inoculated into 1xMinA supplemented with 0.2% glucose, 0.1%
391 casamino acids, 0.1mM $MgSO_4$, and grown to exponential phase. It was then diluted to OD_{600}
392 0.11 in the same media, and 88 µl was added to each well. The plate was incubated at 37℃ with
393 continuous shaking in a FLUOstar Omega (BMG LABTECH, NC) microplate reader. The sample
394 was read every 5 minutes for 24 cycles with excitation and emission wavelengths of 584 nm and
395 620 nm, respectively.
396
397 **Killing kinetics**
398 *E. coli* K12 MG1655 was grown to the exponential phase (OD_{600} ~ 0.3) in 1xMinA supplemented
399 with 0.2% glucose, 0.1% casamino acids, 1 mM $MgSO_4$. The culture was diluted to OD_{600} 0.001
400 (~10^5 CFU/ml) in 1xMinA supplemented with 0.2% glucose, 0.1% casamino acids, 0.1mM
401 $MgSO_4$. One milliliter of bacterial suspension was then mixed with LL-37 (4 µM, 2× MIC), KR-12
402 (8 µM, 2× MIC) or RI-10 (32 µM) and incubated at 37°C. After 15, 30, 60, 90, and 120 minutes
403 of incubation, 50 µl was taken and serially diluted with 1×PBS. Then, 50 µl of the diluted
404 suspension was plated on MH agar Agar plates. The plates were incubated overnight at 37°C
405 for bacterial CFU determination.
406

407 **Membrane depolarization**

408 An overnight culture of *E. coli* K12 MG1655 was inoculated into 1xMinA supplemented with
409 0.2% glucose, 0.1% casamino acids, 1 mM $MgSO_4$, and grown to exponential phase. Bacteria
410 were washed with 1×PBS, re-suspended in twice the volume of 1×PBS containing 25 mM
411 glucose, and incubated at 37°C for 15 minutes. Then, 500 nM (final concentration) of the
412 DiBAC4 (3) bis-(1,3-dibutylbarbituric acid) trimethine oxonol (ANASPEC, CA) was added and
413 vortexed gently. Aliquots of 90 µl of the energized bacteria solution were loaded to the 96 well
414 plates (Corning COSTAR, AZ) and placed in a FLUOstar Omega microplate reader (BMG
415 LABTECH, NC). Fluorescence was read for 15 min at excitation and emission wavelengths of
416 485 nm and 520 nm, respectively. Then, 10 µl of peptide solutions were added and fluorescence
417 readings were recorded for 45 min. Triton X-100 (0.1%) was used as a positive control.

418

419 **Acknowledgments**

420 The authors thank Dr. Mark Goulian for sharing transcriptional reporter strains for *mgrB*, Dr.
421 Nitish Sharma for preparing *ΔmgrB* strains carrying the reporters, and members of the Yadavalli
422 and Wang labs for helpful discussions.

423

424 **Funding**

425 S.S.Y. is supported by the National Institutes of Health - National Institute of General Medical
426 Sciences (NIH-NIGMS) ESI-MIRA R35 GM147566 and institutional start-up funds from Rutgers.
427 A.M. is supported by the Waksman Institute Busch Predoctoral fellowship (2024-25) at Rutgers.
428 G.W. is supported by the NIH/NIAID R56 AI175209. The funders did not play any role in the
429 study design, data collection and analysis, decision to publish, or preparation of the manuscript.

430

431

432

433 **Author contributions**

434 S.S.Y. and G.W. conceived the experiments. All authors planned the experiments, designed the
435 methodology, and performed data analysis. S.A.A., A.F.M., and A.M. performed the
436 experiments. All authors contributed to the writing and editing of the manuscript.

437

438 **Competing interests**

439 The authors declare no competing financial interests.

440

441 **Materials and resource availability**

442 Requests for strains and plasmids generated in this study should be directed to and will be
443 fulfilled by the lead contact, Srujana S. Yadavalli (sam.yadavalli@rutgers.edu). Further
444 information and requests for resources and reagents should be directed to and will be fulfilled by
445 Srujana S. Yadavalli (sam.yadavalli@rutgers.edu) and Guangshun Wang (gwang@unmc.edu).

446

447 **Data availability**

448 The main manuscript and its supporting files include all data generated or analyzed during this
449 study.

450

451 ## References

452 1. M. W. Bader, *et al.*, Recognition of antimicrobial peptides by a bacterial sensor kinase. *Cell* **122**, 461–
453 472 (2005).

454 2. S. S. Yadavalli, *et al.*, Antimicrobial peptides trigger a division block in Escherichia coli through
455 stimulation of a signalling system. *Nat. Commun.* **7**, 12340 (2016).

456 3. E. A. Groisman, The pleiotropic two-component regulatory system PhoP-PhoQ. *J. Bacteriol.* **183**,
457 1835–1842 (2001).

458 4. J. Yuan, F. Jin, T. Glatter, V. Sourjik, Osmosensing by the bacterial PhoQ/PhoP two-component
459 system. *Proc. Natl. Acad. Sci. U. S. A.* **114**, E10792–E10798 (2017).

460 5. S. Matamouros, S. I. Miller, S. Typhimurium strategies to resist killing by cationic antimicrobial
461 peptides. *Biochim. Biophys. Acta* **1848**, 3021–3025 (2015).

462 6. Z. D. Dalebroux, S. I. Miller, Salmonellae PhoPQ regulation of the outer membrane to resist innate
463 immunity. *Curr. Opin. Microbiol.* **17**, 106–113 (2014).

464 7. R. K. Ernst, T. Guina, S. I. Miller, Salmonella typhimurium outer membrane remodeling: role in
465 resistance to host innate immunity. *Microbes Infect.* **3**, 1327–1334 (2001).

466 8. T. Shprung, A. Peleg, Y. Rosenfeld, P. Trieu-Cuot, Y. Shai, Effect of PhoP-PhoQ activation by broad
467 repertoire of antimicrobial peptides on bacterial resistance. *J. Biol. Chem.* **287**, 4544–4551 (2012).

468 9. M. F. Burton, P. G. Steel, The chemistry and biology of LL-37. *Nat. Prod. Rep.* **26**, 1572–1584 (2009).

469 10. D. Vandamme, B. Landuyt, W. Luyten, L. Schoofs, A comprehensive summary of LL-37, the factotum
470 human cathelicidin peptide. *Cell. Immunol.* **280**, 22–35 (2012).

471 11. G. Wang, *et al.*, Design of antimicrobial peptides: Progress made with human cathelicidin LL-37. *Adv.*
472 *Exp. Med. Biol.* **1117**, 215–240 (2019).

473 12. F. Lu, Y. Zhu, G. Zhang, Z. Liu, Renovation as innovation: Repurposing human antibacterial peptide
474 LL-37 for cancer therapy. *Front. Pharmacol.* **13**, 944147 (2022).

475 13. K. Niemirowicz, *et al.*, Magnetic nanoparticles enhance the anticancer activity of cathelicidin LL-37
476 peptide against colon cancer cells. *Int. J. Nanomedicine* **10**, 3843–3853 (2015).

477 14. K. Kuroda, K. Okumura, H. Isogai, E. Isogai, The human cathelicidin antimicrobial peptide LL-37 and
478 mimics are potential anticancer drugs. *Front. Oncol.* **5**, 144 (2015).

479 15. S. Tripathi, *et al.*, Antiviral activity of the human cathelicidin, LL-37, and derived peptides on seasonal
480 and pandemic influenza A viruses. *PLoS One* **10**, e0124706 (2015).

481 16. I. Ginsburg, Bactericidal cationic peptides can also function as bacteriolysis-inducing agents
482 mimicking beta-lactam antibiotics?; it is enigmatic why this concept is consistently disregarded. *Med.*
483 *Hypotheses* **62**, 367–374 (2004).

484 17. Y. Zhang, J. Lakshmaiah Narayana, Q. Wu, X. Dang, G. Wang, Structure and activity of a selective
485 antibiofilm peptide SK-24 derived from the NMR structure of human cathelicidin LL-37.
486 *Pharmaceuticals (Basel)* **14**, 1245 (2021).

487 18. K. A. Henzler Wildman, D.-K. Lee, A. Ramamoorthy, Mechanism of lipid bilayer disruption by the
488 human antimicrobial peptide, LL-37. *Biochemistry* **42**, 6545–6558 (2003).

489 19. J. Turner, Y. Cho, N. N. Dinh, A. J. Waring, R. I. Lehrer, Activities of LL-37, a cathelin-associated
490 antimicrobial peptide of human neutrophils. *Antimicrob. Agents Chemother.* **42**, 2206–2214 (1998).

491 20. A. M. Lippa, M. Goulian, Feedback inhibition in the PhoQ/PhoP signaling system by a membrane
492 peptide. *PLoS Genet.* **5**, e1000788 (2009).

493 21. M. E. Salazar, A. I. Podgornaia, M. T. Laub, The small membrane protein MgrB regulates PhoQ
494 bifunctionality to control PhoP target gene expression dynamics. *Mol. Microbiol.* **102**, 430–445
495 (2016).

496 22. S. S. Yadavalli, *et al.*, Functional determinants of a small protein controlling a broadly conserved
497 bacterial sensor kinase. *J. Bacteriol.* **202** (2020).

498 23. S. Jiang, *et al.*, The inhibitory mechanism of a small protein reveals its role in antimicrobial peptide
499 sensing. *Proc. Natl. Acad. Sci. U. S. A.* **120**, e2309607120 (2023).

500 24. G. Wang, Structures of human host defense cathelicidin LL-37 and its smallest antimicrobial peptide
501 KR-12 in lipid micelles. *J. Biol. Chem.* **283**, 32637–32643 (2008).

502 25. K. Chen, W. Gong, J. Huang, T. Yoshimura, J. M. Wang, The potentials of short fragments of human
503 anti-microbial peptide LL-37 as a novel therapeutic modality for diseases. *Front. Biosci. (Landmark*
504 *Ed.)* **26**, 1362–1372 (2021).

505 26. J. Lakshmaiah Narayana, *et al.*, Origami of KR-12 designed antimicrobial peptides and their potential
506 applications. *Antibiotics (Basel)* **13**, 816 (2024).

507 27. N. Mookherjee, M. A. Anderson, H. P. Haagsman, D. J. Davidson, Antimicrobial host defence
508 peptides: functions and clinical potential. *Nat. Rev. Drug Discov.* **19**, 311–332 (2020).

509 28. S. A. Adeleye, S. S. Yadavalli, Queuosine biosynthetic enzyme, QueE moonlights as a cell division
510 regulator. *PLoS Genet.* **20**, e1011287 (2024).

511 29. T. Miyashiro, M. Goulian, Stimulus-dependent differential regulation in the Escherichia coli PhoQ
512 PhoP system. *Proc. Natl. Acad. Sci. U. S. A.* **104**, 16305–16310 (2007).

513 30. G. Wang, X. Li, Z. Wang, APD3: the antimicrobial peptide database as a tool for research and
514 education. *Nucleic Acids Res.* **44**, D1087-93 (2016).

515 31. K. R. Brink, *et al.*, An E. coli display method for characterization of peptide-sensor kinase
516 interactions. *Nat. Chem. Biol.* **19**, 451–459 (2023).

517 32. G. Wang, *et al.*, Structure, dynamics, and antimicrobial and immune modulatory activities of human
518 LL-23 and its single-residue variants mutated on the basis of homologous primate cathelicidins.
519 *Biochemistry* **51**, 653–664 (2012).

520 33. M. Murakami, B. Lopez-Garcia, M. Braff, R. A. Dorschner, R. L. Gallo, Postsecretory processing
521 generates multiple cathelicidins for enhanced topical antimicrobial defense. *J. Immunol.* **172**, 3070–
522 3077 (2004).

523 34. G. Laverty, S. P. Gorman, B. F. Gilmore, The potential of antimicrobial peptides as biocides. *Int. J.*
524 *Mol. Sci.* **12**, 6566–6596 (2011).

525 35. L. Segev-Zarko, M. L. Mangoni, Y. Shai, “Antimicrobial peptides: multiple mechanisms against a
526 variety of targets” in *Antimicrobial Peptides: Discovery, Design and Novel Therapeutic Strategies*,
527 (CABI, 2017), pp. 119–134.

528 36. R. E. W. Hancock, K. L. Brown, N. Mookherjee, Host defence peptides from invertebrates--emerging
529 antimicrobial strategies. *Immunobiology* **211**, 315–322 (2006).

530 37. T. L. Raguse, E. A. Porter, B. Weisblum, S. H. Gellman, Structure-activity studies of 14-helical
531 antimicrobial beta-peptides: probing the relationship between conformational stability and
532 antimicrobial potency. *J. Am. Chem. Soc.* **124**, 12774–12785 (2002).

533 38. D. L. Lee, R. S. Hodges, Structure-activity relationships of de novo designed cyclic antimicrobial
534 peptides based on gramicidin S. *Biopolymers* **71**, 28–48 (2003).

535 39. J. H. Miller, *A Short Course in Bacterial Genetics*, 1987th Ed. (Cold Spring Harbor Laboratory Press,
536 1992).

537 40. C. A. Schneider, W. S. Rasband, K. W. Eliceiri, NIH Image to ImageJ: 25 years of image analysis.
538 *Nat. Methods* **9**, 671–675 (2012).

539 41. A. Ducret, E. M. Quardokus, Y. V. Brun, MicrobeJ, a tool for high throughput bacterial cell detection
540 and quantitative analysis. *Nat. Microbiol.* **1**, 16077 (2016).

541 42. B. Mishra, T. Lushnikova, R. M. Golla, X. Wang, G. Wang, Design and surface immobilization of short
542 anti-biofilm peptides. *Acta Biomater.* **49**, 316–328 (2017).

543 ## Figure legends

544 **Figure 1. Membrane permeabilization (A-C) and depolarization (D-F) activity of a series of**
545 **LL-37, KR-12, and RI-10 in *E. coli* K-12 MG1655.** The assay was performed in supplemented
546 MinA with 0.1 mM $MgSO_4$. RFU: Relative fluorescence intensity. Data are represented as mean
547 ± range for two independent replicates.

548 **Figure 2. PhoQP-regulated transcription and cell morphology of *E. coli* cells treated with**
549 **sub-MIC levels of antimicrobial peptides. (A)** PhoQP-dependent promoter P_{mgrB}-*yfp* reporter
550 activity, **(B)** phase contrast micrographs, and **(C)** quantification of cell lengths of *E. coli* MG1655
551 (TIM92) cells grown in the presence of sub-MIC levels of antimicrobial peptides LL-37 (1.25
552 μM), KR-12 (5 μM), RI-10 (5 μM), and KE-10 (5 μM). Mean and median values obtained from 4
553 biological replicates are shown in red dots and grey bars, respectively. The number of cells
554 analyzed is indicated by *n*. P-values indicate the results of a Student's t-test: ****P ≤ 0.0001, *P
555 ≤ 0.05, and "ns" = P > 0.05. Scale bar = 5 μm.

556 **Figure 3. PhoQP-regulated transcription and cell morphology of Δ*queE* and Δ*phoQ* cells**
557 **treated with sub-MIC levels of antimicrobial peptides. (A)** Phase contrast micrographs, **(B,**
558 **D)** PhoQP-dependent promoter P_{mgrB}-*yfp* reporter activity, and **(C, E)** quantification of cell
559 lengths of Δ*phoQ* (TIM100) cells and Δ*queE* (SAM31) cells grown in the presence of sub-MIC
560 levels of the antimicrobial peptides LL-37 (1.25 μM), KR-12 (5 μM), RI-10 (5 μM), and KE-10 (5
561 μM). Mean and median values obtained from 4 biological replicates are shown in red dots and
562 grey bars, respectively. The number of cells analyzed is indicated by *n*. P-values indicate the
563 results of a Student's t-test: ****P ≤ 0.0001, ***P ≤ 0.001, *P ≤ 0.05, and "ns" = P > 0.05. Scale
564 bar = 5 μm.

565 **Figure 4. PhoQP-regulated transcription and cell morphology of Δ*mgrB* cells treated with**
566 **sub-MIC levels of antimicrobial peptides. (A)** PhoQP-dependent promoter P_{mgrB}-*yfp* reporter
567 activity in Δ*mgrB* (AML20) cells, **(B)** Phase contrast micrographs, and **(C, D)** quantification of

568 cell lengths of Δ*mgrB* cells and Δ*mgrB* Δ*queE* cells grown in the presence of sub-MIC levels of
569 the antimicrobial peptides LL-37 (1.25 μM), KR-12 (5 μM), RI-10 (5 μM), and KE-10 (5 μM).
570 Mean and median values obtained from 4 biological replicates are shown in red dots and grey
571 bars, respectively. The number of cells analyzed is indicated by *n*. P-values indicate the results
572 of a Student's t-test: ****P ≤ 0.0001, **P ≤ 0.01, *P ≤ 0.05, and "ns" = P > 0.05. Scale bar = 5
573 μm.
574 **Figure 5. Schematic overview of peptide stress response through the *E. coli* PhoQ-PhoP**
575 **signaling system. (A)** At high concentrations, toxic or antimicrobial peptides affect membrane
576 integrity and cause damage, leading to cell death. At sub-MIC levels, both toxic and non-toxic
577 peptides are sensed by the signaling systems, such as PhoQ/PhoP, which control the gene
578 expression under peptide stress, leading to physiological changes, including cell elongation and
579 modification of the outer cell membrane. **(B)** At physiological magnesium concentration, PhoQ is
580 strongly stimulated by specific cationic peptides, and some PhoQ molecules are inhibited by the
581 small protein regulator, MgrB, leading to an intermediate level of PhoQ activation. In the
582 absence of MgrB, PhoQ is not inhibited, and when cells are exposed to peptides, PhoQ is
583 strongly activated, resulting in maximal activation of this signaling system.
584
585
586
587
588
589
590
591
592

593 # Tables and Figures

594

595 **Table 1. Minimum inhibitory concentration (MIC) and minimum bactericidal concentration**
596 **(MBC) values for LL-37 and its derivatives against *E. coli* K-12 MG1655**. MIC values (μM) of
597 antimicrobial peptide LL-37 and its derivatives KR-12, RI-10, and KE-10 against *E. coli* K-12
598 MG1655 in supplemented minimal medium (Min A), Mueller Hinton broth (MHB), and tryptic soy
599 broth (TSB). The corresponding MBC values (μM) are shown within parentheses. Gentamicin is
600 included as a bactericidal antibiotic control. Data represent values obtained from three
601 independent biological replicates.

Strain	Media	LL-37	KR-12	RI-10	KE-10	Gentamicin
E. coli K-12 MG1655	Min A	2 (2)	8-16 (16)	>64 (>64)	>64 (>64)	0.5-1 (1)
	MHB	8 (8)	16-32 (32)	>64 (>64)	>64 (>64)	0.5-1 (1)
	10% MHB	2 (4)	2 (2)	>64 (>64)	>64 (>64)	ND
	TSB	8 (16)	16 (32)	>64 (>64)	>64 (>64)	1-2 (2)
E. coli K-12 MG1655 Δ*mgrB*	Min A	2 (2)	8 (16)	>64 (>64)	>64 (>64)	-
	MHB	8 (8)	8-16 (16)	>64 (>64)	>64 (>64)	-
	10% MHB	2 (2)	2 (2)	>64 (>64)	>64 (>64)	-
	TSB	8-16 (32)	16 (32)	>64 (>64)	>64 (>64)	-

Figure 1

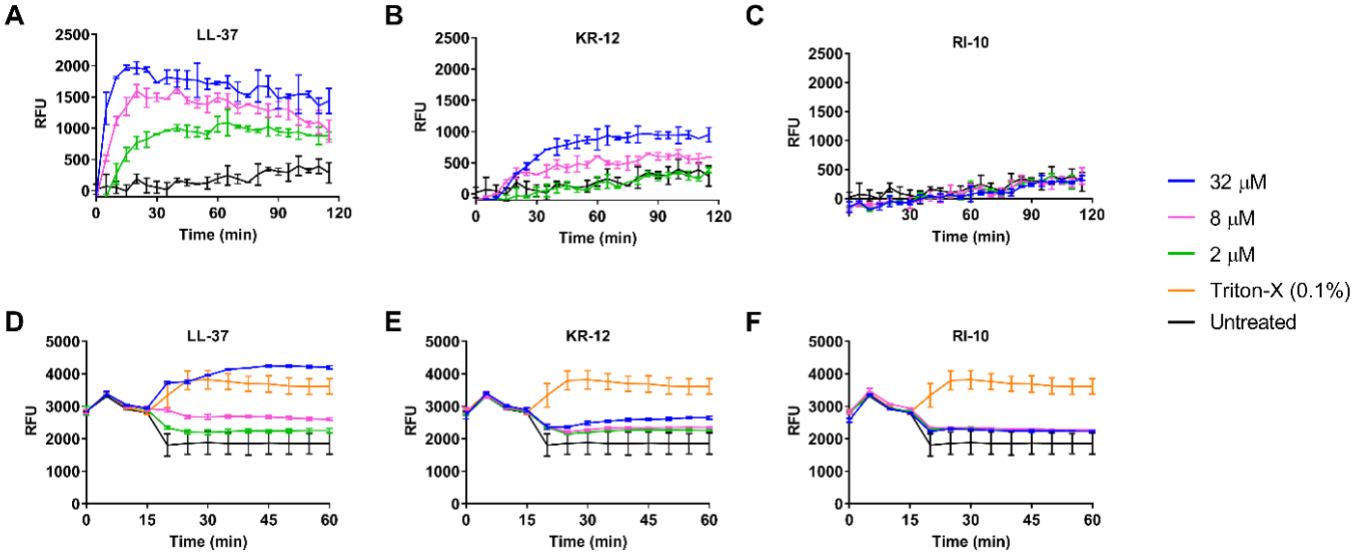
A
LL-37
RFU
Time (min)
B
KR-12
RFU
Time (min)
C
RI-10
RFU
Time (min)
D
LL-37
RFU
Time (min)
E
KR-12
RFU
Time (min)
F
RI-10
RFU
Time (min)
32 μM
8 μM
2 μM
Triton-X (0.1%)
Untreated

Figure 2

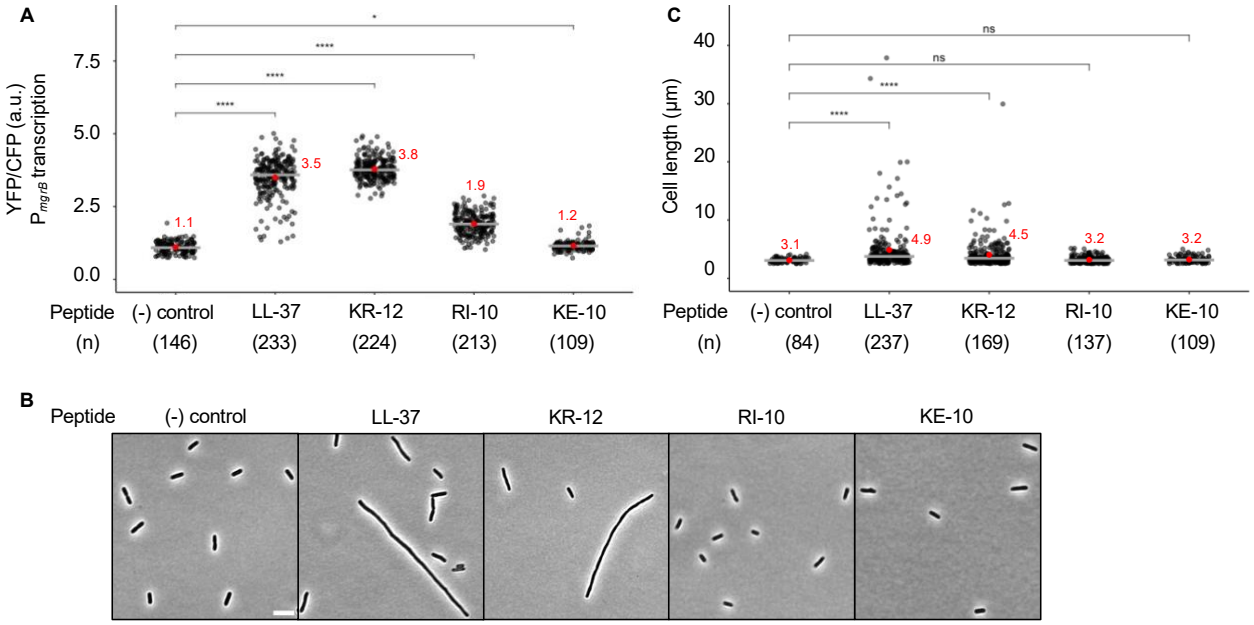
A
YFP/CFP (a.u.)
P_{mgrB} transcription
7.5
5.0
2.5
0.0
1.1
3.5
3.8
1.9
1.2
Peptide
(n)
(-) control
(146)
LL-37
(233)
KR-12
(224)
RI-10
(213)
KE-10
(109)
C
Cell length (µm)
40
30
20
10
0
3.1
4.9
4.5
3.2
3.2
ns
Peptide
(n)
(-) control
(84)
LL-37
(237)
KR-12
(169)
RI-10
(137)
KE-10
(109)
B
Peptide
(-) control
LL-37
KR-12
RI-10
KE-10

Figure 3

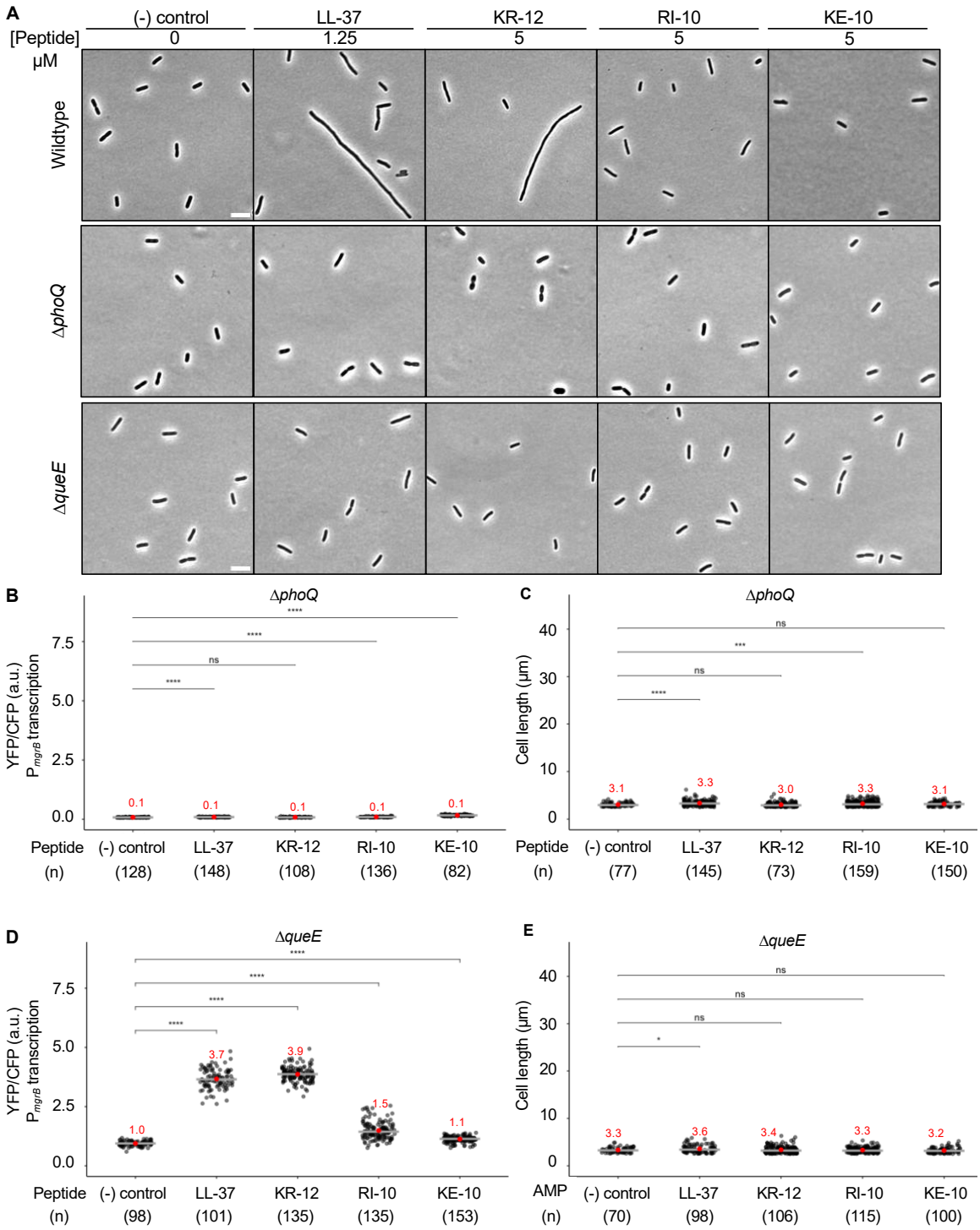
A
(-) control
LL-37
KR-12
RI-10
KE-10
[Peptide] μM
0
1.25
5
5
5
Wildtype
ΔphoQ
ΔqueE
B
ΔphoQ
YFP/CFP (a.u.) P_mgrB transcription
Peptide
(n)
(-) control (128)
LL-37 (148)
KR-12 (108)
RI-10 (136)
KE-10 (82)
C
ΔphoQ
Cell length (μm)
(77)
(145)
(73)
(159)
(150)
D
ΔqueE
(98)
(101)
(135)
(135)
(153)
E
ΔqueE
AMP
(70)
(98)
(106)
(115)
(100)

Figure 4

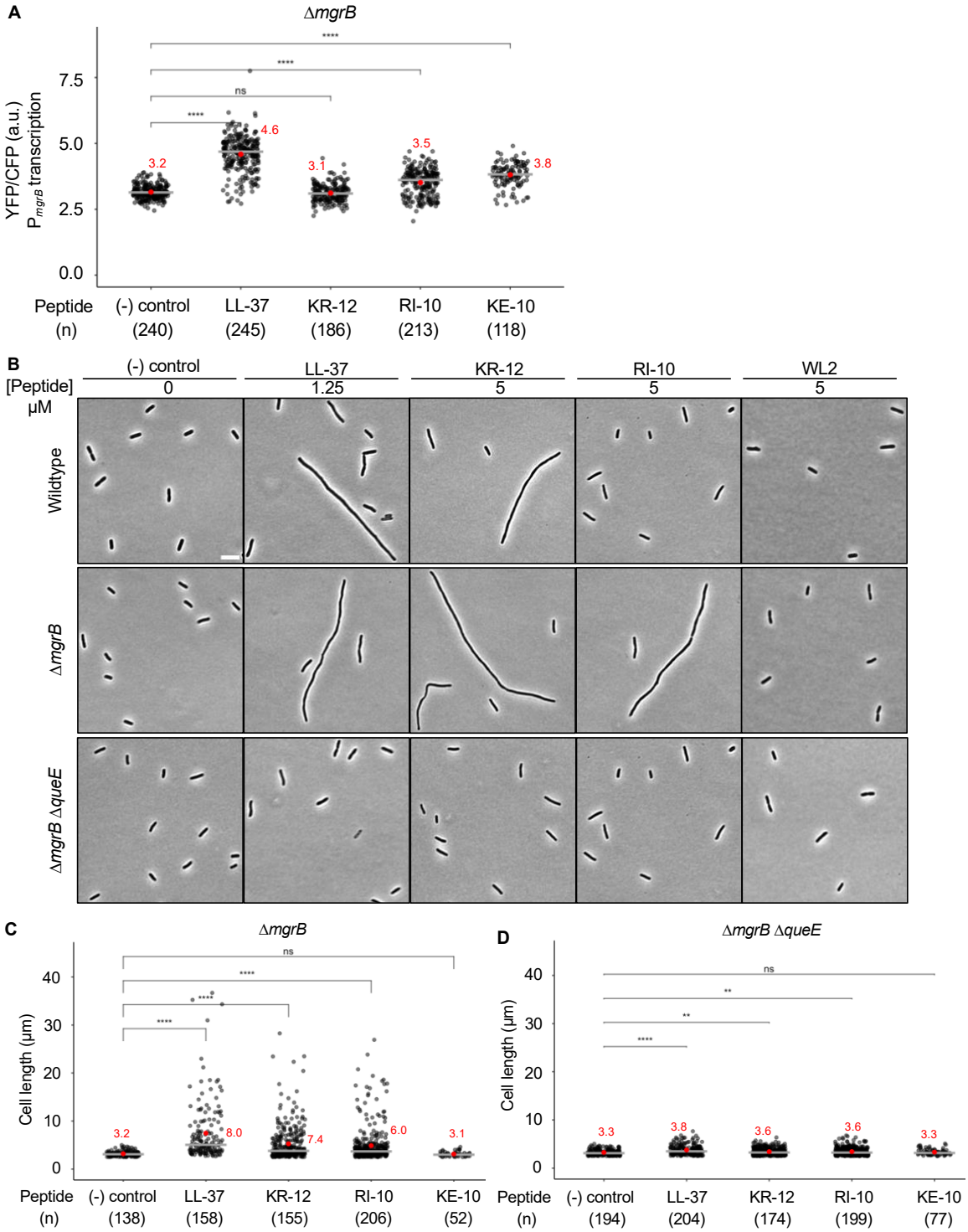
A
ΔmgrB
YFP/CFP (a.u.)
P_mgrB transcription
7.5
5.0
2.5
0.0
****
****
ns
****
3.2
4.6
3.1
3.5
3.8
Peptide
(n)
(-) control
(240)
LL-37
(245)
KR-12
(186)
RI-10
(213)
KE-10
(118)
B
[Peptide]
μM
(-) control
0
LL-37
1.25
KR-12
5
RI-10
5
WL2
5
Wildtype
ΔmgrB
ΔmgrB ΔqueE
C
ΔmgrB
Cell length (μm)
40
30
20
10
0
ns
****
****
****
3.2
8.0
7.4
6.0
3.1
Peptide
(n)
(-) control
(138)
LL-37
(158)
KR-12
(155)
RI-10
(206)
KE-10
(52)
D
ΔmgrB ΔqueE
Cell length (μm)
40
30
20
10
0
ns
**
**
****
3.3
3.8
3.6
3.6
3.3
Peptide
(n)
(-) control
(194)
LL-37
(204)
KR-12
(174)
RI-10
(199)
KE-10
(77)

Figure 5

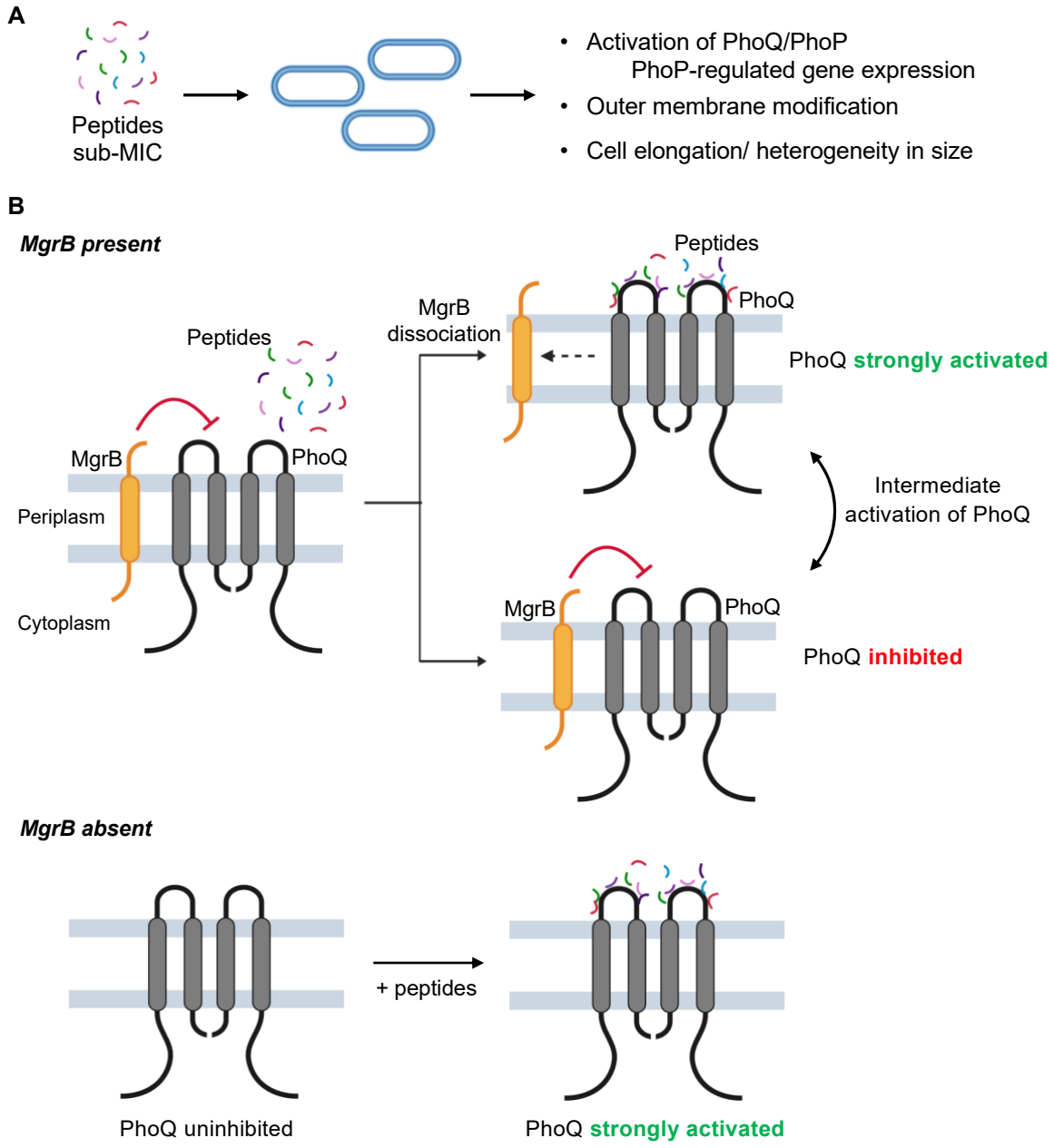
A
Peptides
sub-MIC
• Activation of PhoQ/PhoP
PhoP-regulated gene expression
• Outer membrane modification
• Cell elongation/ heterogeneity in size
B
MgrB present
Peptides
MgrB
PhoQ
Periplasm
Cytoplasm
MgrB
dissociation
Peptides
PhoQ
PhoQ strongly activated
Intermediate
activation of PhoQ
MgrB
PhoQ
PhoQ inhibited
MgrB absent
+ peptides
PhoQ uninhibited
PhoQ strongly activated

Supporting Information

Tables

Table S1. Minimum Inhibitory Concentration (MIC) and Minimum Bactericidal Concentration (MBC) values for LL-37 and its derivatives against *E. coli* strains. MIC values (μM) of antimicrobial peptide LL-37 and its derivatives KR-12 and RI-10 against different *E. coli* strains in supplemented minimal medium (Min A), Mueller Hinton broth (MHB), and tryptic soy broth (TSB). The corresponding MBC values (μM) are shown within parentheses. Data represent values obtained from three independent biological replicates.

***E. coli* strains**	**Media**	**LL-37**	**KR-12**	**RI-10**	**Gentamicin**
E.coli E423-17	Min A	2-4 (4)	8 (8)	>64 (>64)	2 (2)
	MHB	4-8 (8)	32 (32)	>64 (>64)	1 (1)
	TSB	4-8 (8)	32 (>32)	>64 (>64)	2 (4)
E.coli E416-17	Min A	4 (4)	4-8 (8)	>64 (>64)	2 (2)
	MHB	8 (8)	16 (16)	>64 (>64)	1 (2)
	TSB	8-16 (32)	16-32 (32)	>64 (>64)	4 (4)
E.coli 25922	Min A	2-4 (8)	1-2 (16)	>64 (>64)	2 (4)
	MHB	8 (8)	16 (32)	>64 (>64)	1 (2)
	TSB	8 (32)	32 (>32)	>64 (>64)	2-4 (4)

Table S2. List of peptides used in the study.

Peptide	Length	Amino acid sequence	Reference
LL-37	37	LLGDFFRKSKEKIGKEFKRIVQRIKDFLRNLVPRTES	(19)
KR-12	12	KRIVQRIKDFLR	(24)
RI-10	10	RIVQRIKDFL	(3)
KE-10	10	KEKIGKEFKR	(4)

Table S3. List of human LL-37 fragments that share the key recognition sequence for bacterial sensing (bolded).

Name	Peptide amino acid sequence
LL-37	LLGDFFRKSKEKIGKEF**KRIVQRIKDFLR**NLVPRTES
LL-23	LLGDFFRKSKEKIGKEFKRIVQR
LL-29	LLGDFFRKSKEKIGKEF**KRIVQRIKDFLR**
KR-20	**KRIVQRIKDFLR**NLVPRTES
KS-27	KSKEKIGKEF**KRIVQRIKDFLR**NLVPR
KS-30	KSKEKIGKEF**KRIVQRIKDFLR**NLVPRTES
RK-31	RKSKEKIGKEF**KRIVQRIKDFLR**NLVPRTES

Table S4. List of strains used in the study.

Strain	Relevant genotype	Reference/source
E. coli K12 MG1655	*λ⁻ rph-1*	*E. coli* Genetic Stock Center #7740
E. coli E423-17	Clinical antibiotic-resistant isolate	Wang lab, University of Nebraska Medical Center
E. coli E416-17	Clinical antibiotic-resistant isolate	Wang lab, University of Nebraska Medical Center
E. coli 25922	O6 isolate, reference strain for antibiotic susceptibility testing	ATCC
AML20	MG1655 *ΔmgrB* λ_{att} (P_{mgrB}-yfp) HK_{att} (P_{tetA}-*cfp*)	(5)
JNC21	MG1655 *ΔmgrB ΔqueE*::kan λ_{att} (P_{mgrB}-*yfp*) HK_{att} (P_{tetA}-*cfp*). kan^r	(6)
NRS6	MG1655 *ΔmgrB::kan ΔphoQ* λ_{att}::($P_{mgrBt7a}$-*yfp*) HK_{att}::(P_{tetA}-*cfp)*	This work
SAM31	MG1655 *ΔqueE* λ_{att} (P_{mgrB}-*yfp*) HK_{att} (P_{tetA}-*cfp*)	(6)
TIM92	MG1655 λ_{att} (P_{mgrB}-yfp) HK_{att} (P_{tetA}-*cfp*)	(7)
TIM100	MG1655 *ΔphoQ* λ_{att}::(P_{mgrB}-*yfp*) HK_{att}::(P_{tetA}-*cfp)*	(7)
TIM166	MG1655 *ΔphoQ* λ_{att}::($P_{mgrBt7a}$-*yfp*) HK_{att}::(P_{tetA}-*cfp)*	(7)

Figures

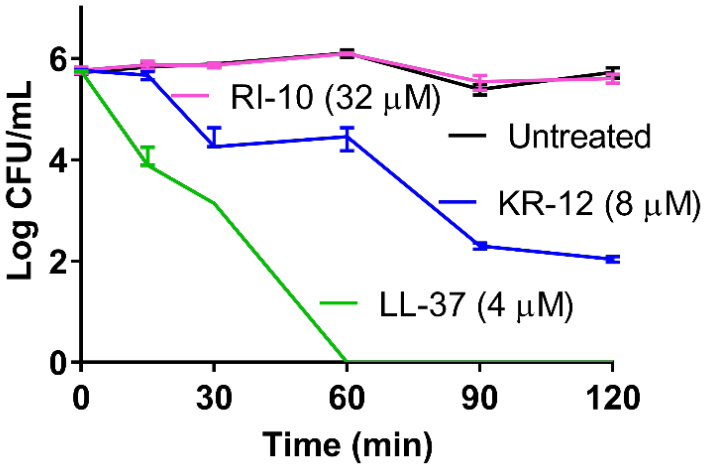

Figure S1. Killing kinetics LL-37, KR-12, and RI-10 against *E. coli* K-12 MG1655. Cells were treated with peptides at indicated concentrations in supplemented MinA with 0.1 mM $MgSO_4$. Data are represented as mean ± range for two biological replicates.

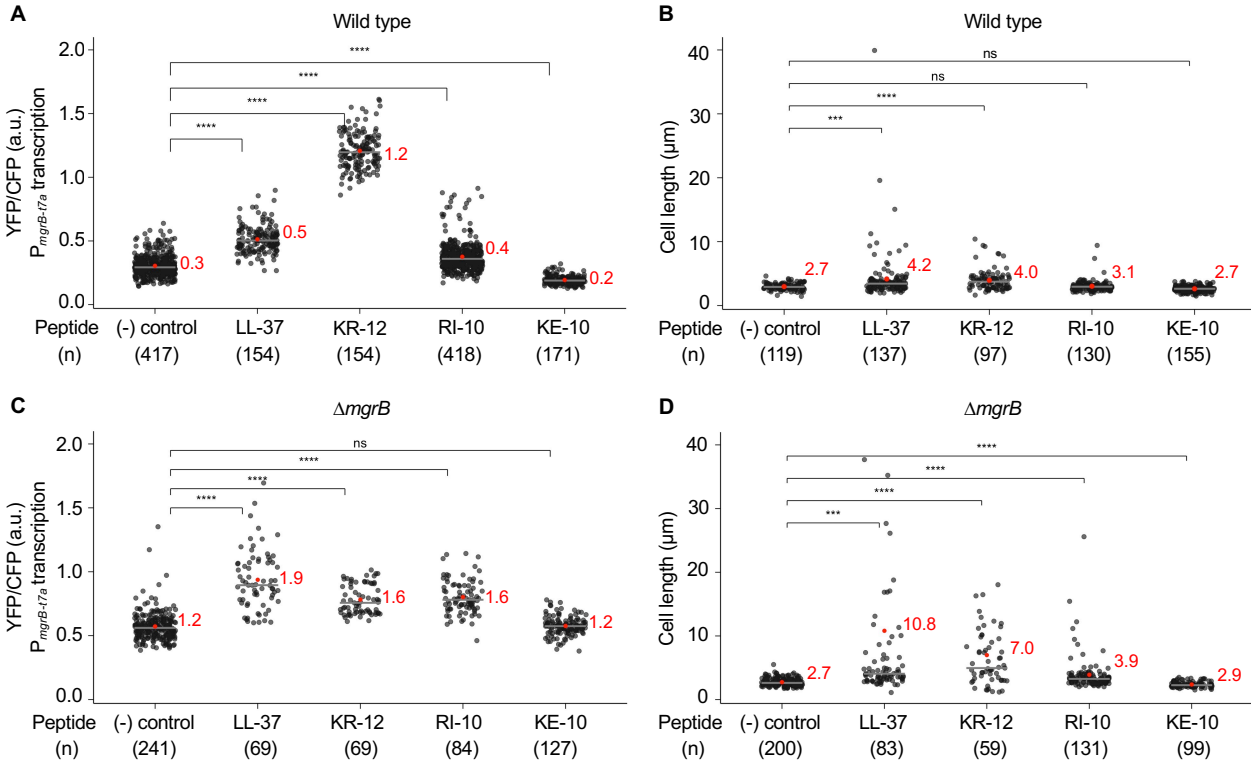

Figure S2. PhoQP-regulated transcription and cell lengths in *phoPQ* and *mgrBt7a* reporter cells treated with sub-MIC levels of antimicrobial peptides. (A, C) PhoQP-dependent promoter reporter activity in wild-type (TIM166) or Δ*mgrB* (NRS6) cells, and **(B, D)** quantification of cell lengths of wild-type or Δ*mgrB* cells, grown in the presence of sub-MIC levels of the antimicrobial peptides LL-37 (1.25 µM), KR-12 (5 µM), RI-10 (5 µM), and KE-10 (5 µM). Mean and median values obtained from 3 biological replicates are shown in red dots and grey bars, respectively. The number of cells analyzed is indicated by *n*. P-values indicate the results of a Student's t-test: ****P ≤ 0.0001, ***P ≤ 0.001, **P ≤ 0.01, *P ≤ 0.05, and "ns" = P > 0.05. Scale bar = 5 µm.

References

1. J. Turner, Y. Cho, N. N. Dinh, A. J. Waring, R. I. Lehrer, Activities of LL-37, a cathelin-associated antimicrobial peptide of human neutrophils. *Antimicrob. Agents Chemother.* **42**, 2206–2214 (1998).

2. G. Wang, Structures of human host defense cathelicidin LL-37 and its smallest antimicrobial peptide KR-12 in lipid micelles. *J. Biol. Chem.* **283**, 32637–32643 (2008).

3. R. F. Epand, G. Wang, B. Berno, R. M. Epand, Lipid segregation explains selective toxicity of a series of fragments derived from the human cathelicidin LL-37. *Antimicrob. Agents Chemother.* **53**, 3705–3714 (2009).

4. A. F. Mechesso, Y. Su, J. Xie, G. Wang, Enhanced antimicrobial screening sensitivity enabled the identification of an ultrashort peptide KR-8 for engineering of LL-37mini to combat drug-resistant pathogens. *ACS Infect. Dis.* **9**, 2215–2225 (2023).

5. A. M. Lippa, M. Goulian, Feedback inhibition in the PhoQ/PhoP signaling system by a membrane peptide. *PLoS Genet.* **5**, e1000788 (2009).

6. S. S. Yadavalli, *et al.*, Antimicrobial peptides trigger a division block in Escherichia coli through stimulation of a signalling system. *Nat. Commun.* **7**, 12340 (2016).

7. T. Miyashiro, M. Goulian, Stimulus-dependent differential regulation in the Escherichia coli PhoQ PhoP system. *Proc. Natl. Acad. Sci. U. S. A.* **104**, 16305–16310 (2007).